Available online at www.sciencedirect.com
SCIENCE DIRECT®
Bioorganic & Medicinal Chemistry 13 (2005) 765–772
Bioorganic & Medicinal Chemistry

Binding of β-D-glucopyranosyl bismethoxyphosphoramidate to glycogen phosphorylase b: kinetic and crystallographic studies

Evangelia D. Chrysina,[a] Magda N. Kosmopoulou,[a] Rozina Kardakaris,[a] Nicolas Bischler,[a] Demetres D. Leonidas,[a] Thanukrishnan Kannan,[c] Duraikkannu Loganathan[c] and Nikos G. Oikonomakos[a,b,*]

[a]*Institute of Organic and Pharmaceutical Chemistry, The National Hellenic Research Foundation, 48 Vassileos Constantinou Ave., 11635 Athens, Greece*
[b]*Institute of Biological Research and Biotechnology, The National Hellenic Research Foundation, 48 Vassileos Constantinou Ave., 11635 Athens, Greece*
[c]*Department of Chemistry, Indian Institute of Technology Madras, Chennai 600 036, India*

Received 6 October 2004; accepted 18 October 2004
Available online 11 November 2004

Abstract—In an attempt to identify a new lead molecule that would enable the design of inhibitors with enhanced affinity for glycogen phosphorylase (GP), β-D-glucopyranosyl bismethoxyphosphoramidate (phosphoramidate), a glucosyl phosphate analogue, was tested for inhibition of the enzyme. Kinetic experiments showed that the compound was a weak competitive inhibitor of rabbit muscle GPb (with respect to α-D-glucose-1-phosphate (Glc-1-P)) with a K_i value of 5.9 (±0.1) mM. In order to elucidate the structural basis of inhibition, we determined the structure of GPb complexed with the phosphoramidate at 1.83 Å resolution. The complex structure reveals that the inhibitor binds at the catalytic site and induces significant conformational changes in the vicinity of this site. In particular, the 280s loop (residues 282–287) shifts 0.4–4.3 Å (main-chain atoms) to accommodate the phosphoramidate, but these conformational changes do not lead to increased contacts between the inhibitor and the protein that would improve ligand binding.

1. Introduction

Inhibitors of glycogen phosphorylase (GP) have been proposed as a therapeutic strategy for improving glycaemic control in type 2 diabetes mellitus and various studies have shown the efficacy of such compounds at lowering blood glucose or inhibiting liver glycogenolysis in vitro or in vivo.[1–6] Inhibitor design for GP targets the catalytic site,[7–16] the AMP allosteric site,[17–22] the inhibitor site[23–25] and a novel allosteric inhibitor site, shown to bind a number of indole-2-carboxamide inhibitors[26–28] and *N*-benzoyl-*N*′-β-D-glucopyranosyl urea.[14] More specifically, the catalytic site has been probed with glucose and glucose analogue inhibitors, designed on the basis of information derived from the crystal structure of T-state GPb.[7–16] The common features of these compounds are that they are highly selective for GP, they are competitive inhibitors with respect to the substrate Glc-1-P, and they bind at the catalytic site and promote the T state (less active) through stabilisation of the closed position of 280s loop (residues 282–287), which blocks access of the substrate glycogen to the catalytic site.

Novel glycosyl phosphoramidates have been recently synthesised as isosteric analogues of glycosyl phosphates[29] aiming to the development of carbohydrate-based therapeutics. In this report we investigated whether β-D-glucopyranosyl bismethoxyphosphoramidate (**1**), an analogue of Glc-1-P, inhibits GP activity. Kinetic studies revealed that the phosphoramidate inhibits muscle GPb with a K_i of 5.9 mM. In order to provide a stereochemical explanation for phosphoramidate inhibition, we have determined the structure of GPb-phosphoramidate complex at 1.83 Å resolution. The structure shows that phosphoramidate binds at the catalytic site and induces substantial conformational changes in the vicinity of the catalytic site.

Keywords: Type 2 diabetes; Glycogen phosphorylase; Phosphoramidate; X-ray crystallography.
* Corresponding author. Tel.: +30 210 7273 761; fax: +30 210 7273 831; e-mail: ngo@eie.gr

0968-0896/$ - see front matter © 2004 Elsevier Ltd. All rights reserved.
doi:10.1016/j.bmc.2004.10.040

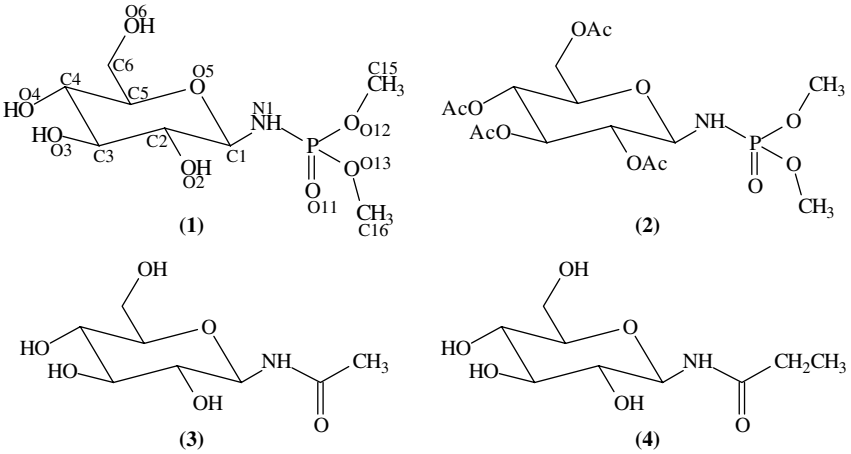

Scheme 1. Chemical structures of phosphoramidate (**1**) (with the numbering system used), its acetylated derivative (**2**), *N*-acetyl-β-D-glucopyranosylamine (**3**) and *N*-propionyl-β-D-glucopyranosylamine (**4**).

2. Materials and methods

The synthesis of phosphoramidate (**1**) (Scheme 1) was described by Kannan et al.[29] Rabbit muscle glycogen phosphorylase b (GPb) was isolated, purified, recrystallised and assayed as described.[10] Kinetic studies performed in the direction of glycogen synthesis in the presence of constant concentrations of glycogen (1% w/v), AMP (1 mM), and various concentrations of Glc-1-P (3–20 mM) and phosphoramidate (2, 5, 7 and 10 mM) showed that the compound exhibited competition (with respect to Glc-1-P) with a K_i of 5.9 ± 0.1 mM.

Native T-state GPb crystals, grown in the tetragonal lattice, space group $P4_32_12$ (as described[30]), were soaked with 150 mM of phosphoramidate for 7.5 h prior to data collection. Diffraction data were collected from a single crystal in room temperature using synchrotron radiation source at Daresbury Laboratory, UK (beamline PX-9.6, $\lambda = 0.87$ Å). Integration of reflections and data reduction was performed using the HKL package.[31]

The crystal structure of GPb-α-D-glucose was used as a starting model for crystallographic refinement against the experimental data applying a standard protocol as implemented by CNS[32] involving rigid body refinement followed by positional and individual B-factor refinement (with bulk solvent correction). $2F_o–F_c$ and $F_o–F_c$ electron density maps were calculated and visualised using the program for molecular graphics 'O'.[33] Both maps indicated that phosphoramidate bound at the catalytic site of GPb inducing conformational changes to residues lining the 280s loop. Additional density at the allosteric site was interpreted as sulfate dianion. The dianion is held by interactions with Arg242, Arg309 and Arg310, and contacts Wat282, which links to Gln71 and Tyr155. Manual rebuilding of the protein structure in the catalytic site as indicated by the electron density maps was then performed. The coordinates of the phosphoramidate model were obtained from the single crystal structure of 2,3,4,6-tetra-*O*-acetyl-β-D-glucopyranosyl bismethoxyphosphoramidate (**2**).[29] The compound was fitted into the additional portion of density observed at the catalytic site after adjustment of the torsion angles. Alternate cycles of refinement and manual fitting of the protein residues and water molecules in the density with the program 'O', improved the quality of the model.

The stereochemistry of the protein residues was validated by PROCHECK.[34,35] Hydrogen bonds and van der Waals interactions were calculated with the program CONTACT as implemented in CCP4[35] applying a distance cut off 3.3 and 4.0 Å, respectively (Tables 2 and 3). The schematic representation of the crystal structures presented in all figures were prepared with the programs MOLSCRIPT[36] and BOBSCRIPT[37] and rendered with RASTER3D.[38] The coordinates of the new structure have been deposited with the RCSB Protein Data Bank (http://www.rcsb.org/pdb) with code: 1XC7.

3. Results and discussion

The phosphoramidate, (**1**), proved to be a weak inhibitor of GPb. Kinetic studies performed at 30 °C and pH 6.8, in the direction of glycogen synthesis, showed that the compound exhibited competitive inhibition (K_i = 5.9 mM) with respect to the substrate Glc-1-P (data not shown). The inhibition by **1** is slightly better than that of the parent sugar, β-D-glucose (K_i = 7.4 mM). Crystallographic data collection processing and refinement statistics for the structure determination of the compound are listed in Table 1. The overall architecture of the T-state GPb with the location of the catalytic site is presented in Figure 1. In the T-state enzyme there is no access for the substrate (glycogen) to the catalytic site; access to this site is partly blocked by the 280s loop (residues 282–287). α-D-Glucose, a competitive inhibitor of the enzyme (K_i = 1.7 mM) that promotes the T state through localisation of the closed position of the 280s loop, binds at this site.[7]

The refined sigmaA weighted $F_o–F_c$ and $2F_o–F_c$ electron density maps clearly indicated binding of phosphoramidate at the catalytic site (Fig. 2), consistent with the

Table 1. Diffraction data and refinement statistics of phosphoramidate in complex with T-state GPb

Data collection and processing statistics	
Experiment	T-state GPb soaked with 150 mM phosphoramidate for 7.5 h
No of images (°)	68 (54.4°)
Space group	$P4_32_12$
Unit cell dimensions	$a = b = 128.7$, $c = 116.2$ $\alpha = \beta = \gamma = 90°$
Resolution (Å)	30.0–1.83
No of observations	616,082
No of unique reflections	84,865 (4137)
R_m (outermost shell)[a]	0.055 (0.479)
Completeness (outermost shell) (%)	98.3 (97.1)
Outermost shell (Å)	1.86–1.83
$\langle I/\sigma(I)\rangle$(outermost shell)[b]	13.2 (3.7)
Multiplicity (outermost shell)	4.5 (4.5)
B-values (Å^2) (Wilson plot)	27.5
Refinement statistics and model quality	
Resolution range (Å)	500.0–1.83
No of reflections used (free)	84,727 (4305)
Residues included	(12–254), (261–314), (324–836)
No of protein atoms	6584
No of water molecules	330
No of heteroatoms	15 (PLP), 18 (phosphoramidate), 5 (SUL)
Final R (R_{free}) (%)[c]	19.3 (21.1)
R (R_{free}) (outermost shell)	25.6 (27.9)
r.m.s.d. in bond lengths (Å)	0.005
r.m.s.d. in bond angles (°)	1.24
r.m.s.d. in dihedral angles (°)	21.5
r.m.s.d. in improper angles (°)	0.79
Average B (Å^2) for residues	(12–254), (261–314), (324–836)
Overall	34.2
C_α, C, N, O	32.1
Side chain	36.2
Average B (Å^2) for heteroatoms	22.3 (PLP), 28.3 (phosphoramidate), 58.4 (SUL)
Average B (Å^2) for water molecules	43.2

[a] $R_m = \sum_i\sum_h | \langle I_h\rangle - I_{ih} | / \sum_i\sum_h I_h$, where $\langle I_h\rangle$and I_{ih} are the mean and the ith measurement of intensity for reflection h, respectively.

[b] $\sigma(I)$ is the standard deviation of I.

[c] Crystallographic $R = \sum || F_o | - | F_c || / \sum | F_o |$, where $|F_o|$ and $|F_c|$ are the observed and calculated structure factor amplitudes, respectively. R_{free} is the corresponding R value for a randomly chosen 5% of the reflections that were not included in the refinement.

kinetic results. There were no changes at the allosteric, the new allosteric site or at the tower/tower helix subunit interface (Fig. 1). In the bound phosphoramidate structure, the torsion angles O5–C1–N1–P, C1–N1–P–O11 and N1–P–O12–C15 are −104.3°, 0.1° and 87.4°, respectively (Fig. 3), so that the conformation of the aglycon moiety about the C1–N1, N1–P and P–O12 bonds is altered from that observed (−81°, −26.3° and 46.6° correspondingly) in the single crystal structure of the fully acetylated derivative,[29] **2**, in order to minimise steric clash with Asn284. The primary hydroxyl group, on the other hand, adopts essentially the same conformation, gauche, (*gg*), in both cases as evident from the torsion angle O5–C5–C6–O6 (−70° for the GPb–phosphoramidate complex and −66.9° for the free compound **2**).

Table 2. Hydrogen bond interactions between phosphoramidate and residues of the catalytic site of GPb

Inhibitor atom	Protein atom	Distance (Å)	Angle (°)
O2	Tyr573 OH	3.1	145.2
	Glu672 OE1	3.2	173.9
	Wat272 O	2.8	—
O3	Glu672 OE1	2.7	119.7
	Ser674 N	3.0	170.1
	Gly675 N	3.1	123.5
O4	Gly675 N	2.8	144.7
	Wat208 O	2.7	—
O6	His377 ND1	2.8	162.9
	Asn484 OD1	2.7	139.7
N1	His377 O	2.9	124.6
O11	Wat109 O	2.8	—

Wat109 O is hydrogen bonded to Asp283 OD1, Asn284 ND2 and Wat207 O. Wat207 in turn is hydrogen bonded to Gly134 N, Gly137 N and Glu88 OE2. Wat272 O is hydrogen bonded to Thr378 OG1, Thr671 O, Ala673 N and Wat271 O. Wat271 O in turn is hydrogen bonded to Val379 N, Thr671 O and Wat270 O. Wat270 O in turn is hydrogen bonded to Gly670 O, Wat279 O and Wat271 O. Wat208 O is hydrogen bonded to Thr676 OG1, PLP O3P and Wat322 O. Wat322 O in turn is hydrogen bonded to PLP O2P and Wat108 O. Wat108 O in turn is hydrogen bonded to Gly135 N, Asp283 OD1 and W107O.

The superposition of the structure of the GPb–phosphoramidate complex with the T-state GPb-α-D-glucose complex structure over well-defined residues (18–249,

Table 3. Van der Waals interactions between phosphoramidate and residues of the catalytic site of GPb

Inhibitor atom	Protein atom	No of contacts
C1	His377 O	1
C2	His377 O; Glu672 OE1; Wat272 O	3
C3	Glu672 OE1; Gly675 N; Wat208 O; Wat322 O	4
C4	Gly675 N; Wat208 O	2
C5	Leu136 N; Wat208 O	2
C6	Gly135 C, O; Leu136 CA; Leu139 CD2; His377 ND1; Asn484 OD1	6
O2	His377 O	1
O3	Glu672 CA, CG, CD, C; Ala673 C, N, CA, CB; Ser674 CA, C; Gly675 CA	11
O4	Asn484 OD1; Ser674 CB, C; Gly675 O, C, CA	6
O5	His377 CB, CG, ND1, O	4
O6	His377 CG, CE1; Leu139 CD2; Val455 CG1, CG2; Asn484 CG	6
N1	His377 CB, C	2
O11	Leu136 CB	1
O12	Leu136 CD1; His377 CB	2
C15	Asp339 OD1; Thr378 CG2; Wat348 O	3
C16	Asp283 O; Phe285 CE1	2
Total		56

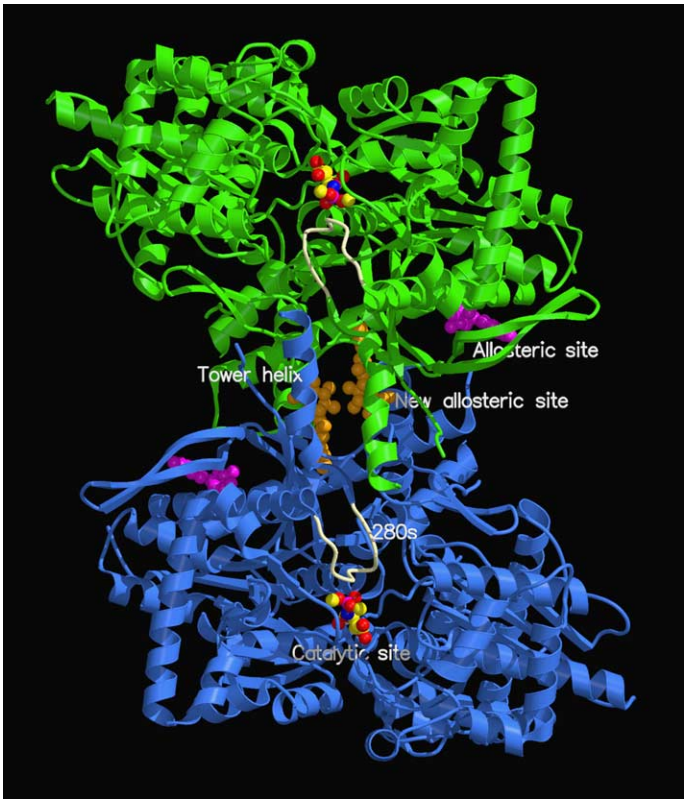

Figure 1. A schematic diagram of the GPb dimeric molecule viewed down the molecular dyad. The positions are shown for the catalytic, allosteric and the new allosteric site. The catalytic site, marked by phosphoramidate, shown in ball-and-stick representation, is buried at the centre of the subunit and is accessible to the bulk solvent through a 15-Å-long channel. Upon binding of phosphoramidate to the enzyme, there is a significant rearrangement of the 280s loop (shown in cream) within the catalytic site. The allosteric site, which binds the weak activator IMP (shown in magenta), is situated at the subunit–subunit interface some 30 Å from the catalytic site. The new allosteric inhibitor site, located inside the central cavity, formed on association of the two subunits, binds indole-2 carboxamide analogues, *N*-benzoyl-*N*-β-D-glucopyranosyl urea (shown in orange). The position of the tower helix (residues 262–276) is also indicated.

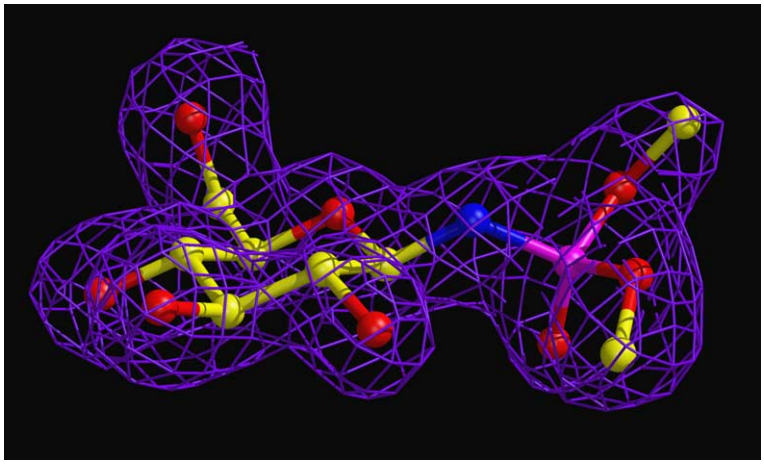

Figure 2. SigmaA-weighted $2F_o$–F_c electron density map of the refined phosphoramidate structure bound at the catalytic site of GPb. The map is contoured at 1.0 σ level.

262–312 and 326–829) gave an r.m.s. deviation of 0.254 Å for Cα atoms, indicating that the complexes are overall similar. The glucopyranose moiety, of phosphoramidate, is located in a position similar to that previously reported for α-D-glucose,[7] while the ligand β-substituent occupies the so-called β-pocket, a side channel from the catalytic site, directed towards residue His341, but with no access to the bulk solvent. The hydrogen bonding network (Table 2) to the peripheral hydroxyls of the glucopyranose moiety is analogous to that observed for the α-D-glucose. In specific, O2 is hydrogen bonded to Tyr573 OH, Glu672 OE1 and the

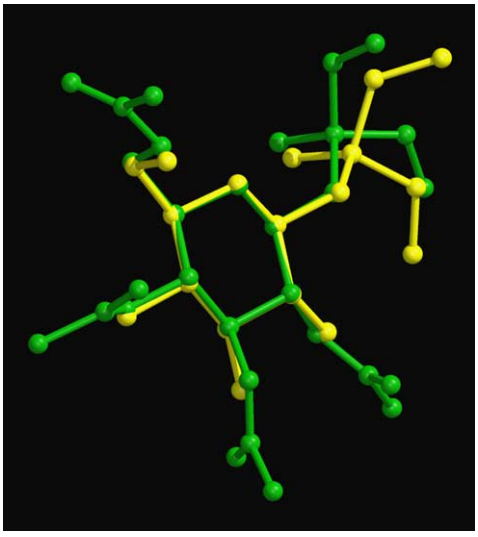

Figure 3. Superposition of the acetylated phosphoramidate structure as defined by small molecule X-ray crystallography (shown in green) with the phosphoramidate (shown in yellow) when bound at the catalytic site of GPb.

side chain OG1 of Thr378 as well as the main chain atoms of Thr671 (O) and Ala673 (N) through a water mediated interaction by Wat272. Wat272 is present in the GPb-α-D-glucose complex (Wat146) but appears to have shifted by ~0.8 Å in the GPb–phosphoramidate structure. However, there is no hydrogen bond between O2 and Asn284 ND2 of the 280s loop, which undergoes conformational change (see below). O3 is forming hydrogen bond interactions with both Glu672 OE1 and Ser674 N as in the GPb-α-D-glucose complex and an additional hydrogen bond with Gly675 N while O4 and O6 maintain their interactions with Gly675 N, Wat208 and His377 ND1, Asn484 OD1, respectively, in both complex structures (Fig. 4). The atomic positions of C1, C2, C5, O5 are slightly changed in the GPb–phosphoramidate structure (compared to those of α-D-glucose) and exhibit shifts of ~0.5–0.6 Å (Fig. 5). O11, of the bismethoxyphosphoramidate substituent, is forming no direct hydrogen bond interactions with the residues lining the catalytic site, however, it stabilises the new conformation of the 280s loop through water-mediated (Wat109) interactions with the side chains of Asp283 OD1 and Asn284 ND2. O11 is also interacting with backbone N atoms of the residues of the glycine-rich helix (residues 130–137) Gly134 and Gly137 as well as the side chain OE2 of Glu88. Wat109 (Wat233 in the GPb-α-D-glucose complex) appears to have shifted significantly (~1.6 Å) compared to its former position in the GPb-α-D-glucose complex since otherwise it would form very close interactions with O11 (~1.6 Å). N1 of phosphoramidate is hydrogen bonded to His377 O, an interaction which is present in all β-D-glucopyranosylamine[4,16] and spirohydantoin analogues of β-D-glucopyranose (Watson et al., unpublished results). O12 and O13 atoms bonded to the phosphorus atom do not form any polar interactions (Fig. 4). The overall water structure at the catalytic site has been maintained (as compared to the GPb-α-D-glucose complex) with the exception of water molecules Wat272 and Wat109 that have shifted, in order to form more favourable interactions with the ligand, and Wat12 that was displaced in order to avoid clashes with C15 ligand atom.

The closed conformation of the 280s loop in the T-state enzyme has been well documented from a series of crystallographic studies of GP in complex with a plethora of glucose analogues.[4] Recently, it was shown that this flexible loop shifts 1.3–1.7 Å (Ca atoms) on binding of *N*-benzoyl-*N*′-β-D-glucopyranosyl urea[14] in order to accommodate the ligand. In the present study, a new conformational motif of the 280s loop was observed, on phosphoramidate binding, at the catalytic site. In specific, the main chain atoms of the residues of the 280s loop shift as follows: Asn282 (0.8–3.0 Å), Asp283 (1.2–2.5 Å), Asn284 (3.1–4.3 Å), Phe285 (0.6–1.7 Å), Phe286 (0.3–0.5 Å) and Glu287 (0.3–0.4 Å). The most remarkable shifts of the backbone atoms are observed for residues Asn282, Asp283 and Asn284. In particular, the shift of Asn282 resulted in a change of

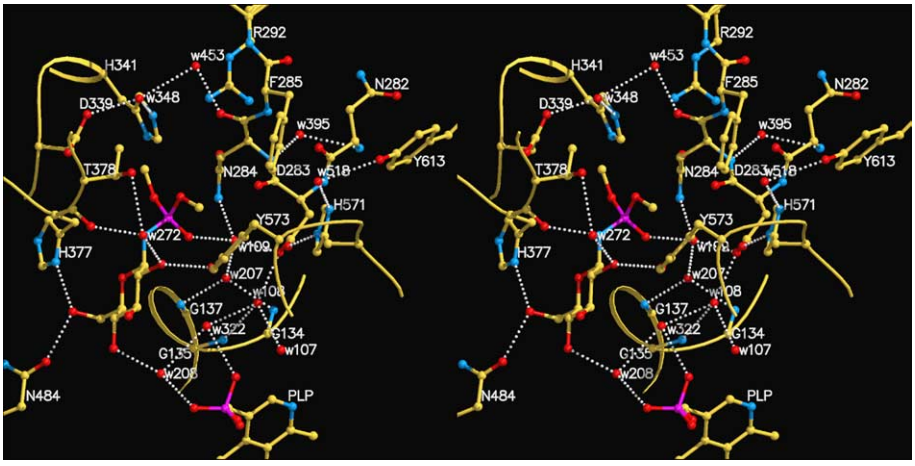

Figure 4. Stereo representation of the molecular interactions of phosphoramidate when bound at the catalytic site of GPb. Water molecules are labelled as w. Residues 88, and 671–676 are not shown for reasons of clarity.

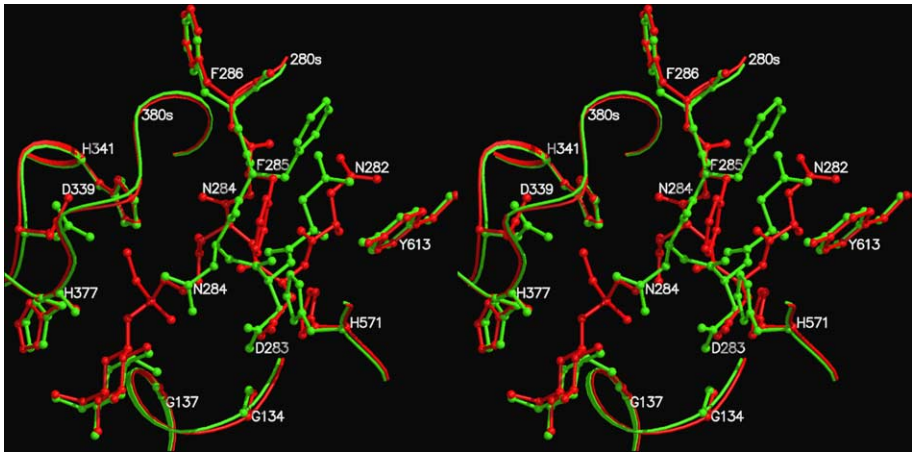

Figure 5. Stereo diagram of the structures of GPb in complex with glucose (shown in green) and with phosphoramidate (shown in red). Residues 88, and 671–676 are not shown for reasons of clarity.

the dihedral χ_3 (C_β–C_γ–C_δ–$O_{\varepsilon 1}$) of Glu287 in order to maintain the hydrogen bond interaction between Asn282 ND2 and Glu287 OE2 (~2.7 Å) (3.3 Å in the GPb-α-D-glucose structure). In addition, a new hydrogen bond between Asn282 O and Phe285 N (~3.0 Å) stabilises the new conformation. Apart from the main chain atoms, the side chain of Asp283 also changes significantly. Thus, dihedral χ_2 (C_α–C_β–C_γ–$O_{\delta 1}$) rotates by ~74° to satisfy the stereochemistry conditions imposed by Asn284 conformational changes (shifts of backbone atoms and rotation of side chain dihedral χ_2 by ~142°) (Fig. 5).

In the GPb–phosphoramidate complex, the conformational change of the side chain of Asp283 was followed by a rotation of the imidazole ring (dihedral angle χ_1 of His571 rotates ~27°). The water molecule Wat108 (W85 in GPb-α-D-glucose) also shifts by ~1.0 Å to maintain its hydrogen bond with the carboxyl oxygen of Asp283 OD1, and Wat109 (Wat233 in GPb-α-D-glucose) moves by 1.6 Å to mediate the hydrogen bonding interactions of the ligand and the side chain of Asp283. The new position of Asn284 creates more space in order for the ligand to be accommodated at the catalytic site, causing displacement of two water molecules Wat143 and Wat302 (numbering from GPb-α-D-glucose complex) and a shift of Wat395 (Wat124 of GPb-α-D-glucose), that mediates the hydrogen bond interaction of Asn284 OD1 and the backbone nitrogen of Asn282, by ~1.8 Å. In its new position Asn284 is hydrogen bonded (through OD1 and ND2) to OE1 of Glu88.

In the native T state GPb, and the GPb-α-D-glucose complex Phe285 is stacked close to Tyr613 and together these two hydrophobic aromatic residues form the inhibitor site, a site that binds caffeine and a number of other fused ring compounds.[4] In the GPb–phosphoramidate complex the side chain (χ_1) of Phe285 is rotated by ~100°. The new orientation of Phe285 with concomitant changes in the adjacent His571, described above, result in a destruction of the inhibitor site. In fact, His571 approaches Phe285 and there are now extensive contacts between CE1 of His571 and the atoms of the aromatic ring of Phe285 (Fig. 5). In general the rearrangement of the 280s loop within the catalytic site on binding phosphoramidate does not lead to increased contacts between the inhibitor and the protein as in the case of the *N*-benzoyl-*N*′-β-D-glucopyranosyl urea binding. The strong affinity (K_i = 4.6 μM) of the latter compound for GPb could be interpreted in terms of its extensive interactions with the protein.[14] Also, in the GPb–phosphoramidate complex, the plane of the carboxyl group of Asp339 has flipped 90° about the CB–CG bond with respect to its position in the GPb-α-D-glucose complex, which would place C15 atom close to the carboxyl group of Asp339.

It is concluded that the restructuring of the 280s loop, the small adjustments of the glucopyranose moiety, the residues of the catalytic site and water structure, needed to accommodate the ligand substituent, would presumably have an energetic cost, in addition to the loss of energy during desolvation, perhaps explaining the low affinity of phosphoramidate for the enzyme.

Among the amido sugar derivatives evaluated till date, *N*-acetyl-β-D-glucopyranosylamine (**3**) is the best inhibitor (K_i = 0.032 mM) and the next best being the corresponding β-1-*N*-propionamido derivative (**4**, K_i = 0.039 mM). A comparative analysis of the crystal structures of GPb complexes of these two carboxamido derivatives reported earlier[11] with that of phosphoramidate (**1**) in terms of aglycon conformation and network of hydrogen bonding and van der Waals interactions reveals the following important similarities. Values of the N-glycosidic torsion angle O5–C1–N1–P observed are −98°, −92° and −104.3° for the GPb complexes of **3**, **4** and **1**, respectively. Incidentally, comparable values, −93.8°[39] and −89.5°[40] have been reported for the free forms of **3** and **4** indicating that the conformation about the N-glycosidic bond has not been influenced much by the binding forces acting at the catalytic site. Moreover, in all three complexes, N1 is hydrogen bonded to His377 O and this is an essential feature contributing approximately 1.7 kcal/mol to the binding energy.[11] In contrast, the three complexes do differ in the number of polar

contacts and van der Waals interactions between GPb and the aglycon atoms (3 polar and 15 nonpolar for **3**, 3 polar and 16 nonpolar in **4** and 2 polar and 10 nonpolar in **1**).

In summary, the lesser number of these interactions observed in the GPb–phosphoramidate complex and the steric bulk of the aglycon moiety inducing unfavourable conformational alterations in the 280's loop appear to have led to decreased affinity. Thus the present study aimed at examining the inhibition of GPb by β-D-glucopyranosyl bismethoxyphosphoramidate has demonstrated that this novel analogue of the substrate Glc-1-P is a competitive inhibitor albeit with low affinity. The present findings strengthen the earlier observations that a relatively bulky β-anomeric substituent leads to diminished binding. Further work to examine appropriately modified analogues with greater potency is currently in progress.

Acknowledgements

This work was supported by Greek GSRT through PENED-204/2001, ENTER-EP6/2001 and the SRS Daresbury Laboratory through the (IHPP HPRI-CT-1999-00012). We also wish to acknowledge the assistance of the staff at SRS for providing excellent facilities for X-ray data collection. Funding provided by the Council of Scientific and Industrial Research, New Delhi is gratefully acknowledged.

References and notes

1. McCormack, J. G.; Westergaard, N.; Kristiansen, M.; Brand, C. L.; Lau, J. *Curr. Pharm. Des.* **2001**, *7*, 1451.
2. Somsák, L.; Kovács, L.; Tóth, M.; Ősz, E.; Szilágyi, L.; Györgydeák, Z.; Dinya, Z.; Docsa, T.; Tóth, B.; Gergely, P. *J. Med. Chem.* **2001**, *44*, 2843.
3. Treadway, J. L.; Mendys, P.; Hoover, D. J. *Exp. Opin. Invest. Drugs* **2001**, *10*, 439.
4. Oikonomakos, N. G. *Curr. Protein Pept. Sci.* **2002**, *3*, 561.
5. Kurukulasuriya, R.; Link, J. T.; Madar, D. J.; Pei, Z.; Richards, S. J.; Rohde, J. J.; Souers, A. J.; Szczepankiewicz, B. G. *Curr. Med. Chem.* **2003**, *10*, 123.
6. Somsák, L.; Nagy, V.; Hadady, Z.; Docsa, T.; Gergely, P. *Curr. Pharm. Des.* **2003**, *9*, 1177.
7. Martin, J. L.; Veluraja, K.; Johnson, L. N.; Fleet, G. W. J.; Ramsden, N. G.; Bruce, I.; Oikonomakos, N. G.; Papageorgiou, A. C.; Leonidas, D. D.; Tsitoura, H. S. *Biochemistry* **1991**, *30*, 10101.
8. Watson, K. A.; Mitchell, E. P.; Johnson, L. N.; Son, J. C.; Bichard, C. J. F.; Orchard, M. G.; Fleet, G. W. J.; Oikonomakos, N. G.; Leonidas, D. D.; Kontou, M.; Papageorgiou, A. C. *Biochemistry* **1994**, *33*, 5745.
9. Bichard, C. J. F.; Mitchell, E. P.; Wormald, M. R.; Watson, K. A.; Johnson, L. N.; Zographos, S. E.; Koutra, D. D.; Oikonomakos, N. G.; Fleet, G. W. J. *Tetrahedron Lett.* **1995**, *36*, 2145.
10. Oikonomakos, N. G.; Kontou, M.; Zographos, S. E.; Watson, K. A.; Johnson, L. N.; Bichard, C. J. F.; Fleet, G. W. J.; Acharya, K. R. *Protein Sci.* **1995**, *4*, 2469.
11. Watson, K. A.; Mitchell, E. P.; Johnson, L. N.; Cruciani, G.; Son, J. C.; Bichard, C. J. F.; Fleet, G. W. J.; Oikonomakos, N. G.; Kontou, M.; Zographos, S. E. *Acta Crystallogr.* **1995**, *D51*, 458.
12. Gregoriou, M.; Noble, M. E. M.; Watson, K. A.; Garman, E. F.; Krulle, T. M.; Fuente, C.; Fleet, G. W. J.; Oikonomakos, N. G.; Johnson, L. N. *Protein Sci.* **1998**, *7*, 915.
13. Fosgerau, K.; Westergaard, N.; Quistorff, B.; Grunnet, N.; Kristiansen, M.; Lundgren, K. *Arch Biochem. Biophys.* **2000**, *380*, 274.
14. Oikonomakos, N. G.; Kosmopoulou, M.; Zographos, S. E.; Leonidas, D. D.; Chrysina, E. D.; Somsák, L.; Nagy, V.; Praly, J.-P.; Docsa, T.; Tóth, B.; Gergely, P. *Eur. J. Biochem.* **2002**, *269*, 1984.
15. Oikonomakos, N. G.; Skamnaki, V. T.; Ősz, E.; Szilágyi, L.; Somsák, L.; Docsa, T.; Tóth, B.; Gergely, P. *Bioorg. Med. Chem.* **2002**, *10*, 261.
16. Chrysina, E. D.; Oikonomakos, N. G.; Zographos, S. E.; Kosmopoulou, M. N.; Bischler, N.; Leonidas, D. D.; Kovács, L.; Docsa, T.; Gergely, P.; Somsák, L. *Biocatal. Biotransform.* **2003**, *21*, 233.
17. Zographos, S. E.; Oikonomakos, N. G.; Tsitsanou, K. E.; Leonidas, D. D.; Chrysina, E. D.; Skamnaki, V. T.; Bischoff, H.; Goldman, S.; Schram, M.; Watson, K. A.; Johnson, L. N. *Structure* **1997**, *5*, 1413.
18. Oikonomakos, N. G.; Tsitsanou, K. E.; Zographos, S. E.; Skamnaki, V. T.; Goldmann, S.; Bischoff, H. *Protein Sci.* **1999**, *8*, 1930.
19. Lu, Z.; Bohn, J.; Bergeron, R.; Deng, Q.; Ellsworth, K. P.; Geissler, W. M.; Harris, G.; McCann, P. E.; McKeever, B.; Myers, R. W.; Saperstein, R.; Willoughby, C. A.; Yao, J.; Chapman, K. *Bioorg. Med. Chem. Lett.* **2003**, *13*, 4125.
20. Ogawa, A. K.; Willoughby, C. A.; Bergeron, R.; Ellsworth, K. P.; Geissler, W. M.; Myers, R. W.; Yao, J.; Harris, G.; Chapman, K. T. *Bioorg. Med. Chem. Lett.* **2003**, *13*, 3405.
21. Rosauer, K. G.; Ogawa, A. K.; Willoughby, C. A.; Ellsworth, K. P.; Geissler, W. M.; Myers, R. W.; Deng, Q.; Chapman, K. T.; Harris, G.; Moller, D. E. *Bioorg. Med. Chem. Lett.* **2003**, *13*, 4385.
22. Kristiansen, M.; Andersen, B.; Iversen, L. F.; Westergaard, N. *J. Med. Chem.* **2004**, *47*, 3537.
23. Oikonomakos, N. G.; Schnier, J. B.; Zographos, S. E.; Skamnaki, V. T.; Tsitsanou, K. E.; Johnson, L. N. *J. Biol. Chem.* **2000**, *275*, 34566.
24. Tsitsanou, K. E.; Skamnaki, V. T.; Oikonomakos, N. G. *Arch. Biochem. Biophys.* **2000**, *384*, 245.
25. Ekstrom, J. L.; Pauly, T. A.; Carty, M. D.; Soeller, W. C.; Culp, J.; Danley, D. E.; Hoover, D. J.; Treadway, J. L.; Gibbs, E. M.; Fletterick, R. J.; Day, Y. S.; Myszka, D. G.; Rath, V. L. *Chem. Biol.* **2002**, *9*, 915.
26. Oikonomakos, N. G.; Skamnaki, V. T.; Tsitsanou, K. E.; Gavalas, N. G.; Johnson, L. N. *Structure* **2000**, *8*, 575.
27. Rath, V. L.; Ammirati, M.; Danley, D. E.; Ekstrom, J. L.; Gibbs, E. M.; Hynes, T. R.; Mathiowetz, A. M.; McPherson, R. K.; Olson, T. V.; Treadway, J. L.; Hoover, D. J. *Chem. Biol.* **2000**, *7*, 677.
28. Oikonomakos, N. G.; Zographos, S. E.; Skamnaki, V. T.; Archontis, G. *Bioorg. Med. Chem.* **2002**, *10*, 1313.
29. Kannan, T.; Vinodhkumar, S.; Varghese, B.; Loganathan, D. *Bioorg. Med. Chem. Lett.* **2001**, *11*, 2433.
30. Oikonomakos, N. G.; Melpidou, A. E.; Johnson, L. N. *Biochim. Biophys. Acta* **1985**, *832*, 248.
31. Otwinowski, Z.; Minor, W. *Methods Enzymol.* **1997**, *276*, 307.
32. Brünger, A. T.; Adams, P. D.; Clore, G. M.; DeLano, W. L.; Gros, P.; Grosse-Kunstleve, R. W.; Jiang, J.-S.; Kuszewski, J.; Nilges, M.; Pannu, N. S.; Read, R. J.; Rice, L. M.; Simonson, T.; Warren, G. L. *Acta Crystallogr.* **1998**, *D54*, 905.

33. Jones, T. A.; Zou, J. Y.; Cowan, S. W.; Kjeldgaard, M. *Acta Crystallogr.* **1991**, *A47*, 110.
34. Laskowski, R. A.; MacArthur, M. W.; Moss, D. S.; Thornton, J. M. *J. Appl. Crystallogr.* **1993**, *26*, 283.
35. CCP4. *Acta Crystallogr.* **1994**, D50, 760.
36. Kraulis, P. *J. Appl. Crystallogr.* **1991**, *24*, 946.
37. Esnouf, R. M. *J. Mol. Graphics Modelling* **1997**, *15*, 132.
38. Merritt, E. A.; Bacon, D. J. *Methods Enzymol.* **1997**, *277*, 505.
39. Sriram, D.; Srinivasan, H.; Srinivasan, S.; Priya, K.; VishnuThirtha, M.; Loganathan, D. *Acta Crystallogr. Sect C: Struct. Commun.* **1997**, *C53*, 1075.
40. Lakshmanan, T.; Priya, K.; Sriram, D.; Loganathan, D. *Biochem. Biophys. Res. Commun.* **2003**, *312*, 405.